Journal of Applied Research in Science and Humanities

Analytical investigation of peristaltic flow of non-Newtonian fluid in a vertical nonuniform channel with heat and mass transfer: Applications to physiological systems

Hamed Mahmoud Sayed[1], **Abdelrahman Mohamed Abdelazez**, **Ahmed Saeed Saied**, **Abdelrahman Yaser Abrahem**, **Hesham Tarek Abdelmoula**, **Mahmoud Mostafa Hamza**, **Mohamed Khaled Yuosef**, **and Rawan Abdulah Abdelfatah**

Department of Mathematics, Faculty of Education, Ain Shams University, Roxy, Cairo, Egypt

Abstract

This study investigates the impact of heat and mass transfer on the magnetohydrodynamic oscillatory flow of a non-Newtonian fluid (Casson fluid) in a wavy channel embedded in a porous medium, taking into consideration the influence of the heat source or sink, thermal radiation, suction or injection, and chemical reaction. To obtain analytical solutions to the dimensionless governing equations, we utilize the command (DSolve) from Wolfram Mathematica 14. The influence of different physical parameters on the momentum, energy, and concentration profiles of the Casson fluid is analyzed. Consequently, the mathematical findings remain displayed graphically.

Keywords

Casson fluid, Oscillatory flow, Porous channel, Magnetic field, chemical reaction

Nomenclature

u' Axial velocity

p' Fluid pressure

x' , y' Spatial coordinates

[1] Corresponding author. E-mail: hamedali@edu.asu.edu.eg

T_0, T_1 Reference fluid temperatures

C_0, C_1 Reference fluid concentrations

b Amplitude of the wavy walls

2d Channel width

a Amplitude ratios

λ^* Wavelength

c Propagation velocity

H_1, H_2 Channel walls

h_1, h_2 Dimensionless channel walls

u Nondimensional velocity

p Dimensionless fluid pressure

v_0 Constant horizontal velocity

B_0 Magnetic field intensity

K Thermal conductivity of the fluid

D Mass diffusivity

Cp Specific heat at constant pressure

T' Temperature of fluid

C' Concentration of fluid

t' Time

g Acceleration due to gravity

k* Porous permeability

Ha Hartmann number

S Suction/injection parameter

Pr Prandtl number

Da Darcy number

G_t Thermal Grashof number

G_c Solutal Grashof number

Nr Thermal radiation parameter

Kr Chemical reaction parameter

Sc Schmidt number

Q Heat source/sink parameter

Greek Symbols

μ Viscosity of fluid

λ Dimensionless pressure gradient

α Mean radiation absorption coefficient

ω Frequency of oscillation

β Casson fluid parameter

ρ Density of fluid

φ Phase difference

θ Dimensionless temperature

ϕ Dimensionless concentration

σ Fluid conductivity

β_T Thermal expansion coefficient

β_c Solutal expansion coefficient

1. Introduction

The engineering and scientific communities often work with fluids such as air, water, and oil that exhibit Newtonian behavior under normal conditions. However, in certain transient flow scenarios, non-Newtonian fluids are important. These scenarios can be found in various industries such as chemical processing, plastics manufacturing, and the mining industry where slurries and mud are frequently handled. Additionally, non-Newtonian behavior is observed in fields such as tissue engineering, pipeline industry, lubrication, and biomedical transport. Therefore, simulating events involving non-Newtonian fluid flow is crucial for these industries. Recent advancements in polymer manufacturing and biofluid dynamics have led to increased interest in non-Newtonian fluid flow through tubes with a fixed yield value.

The Casson fluid is commonly used for this purpose, as it is a liquid that has shear thinning properties and an infinite viscosity with zero yield stress and infinite shear rate. In many fields, such as the flow of blood through arteries, the working of magnetohydrodynamic (MHD) generators, and extraction activities in geothermal energy fields, the magnetohydrodynamic oscillatory flow of highly viscous fluids is of interest. Various researchers have studied oscillatory

flows of both Newtonian and non-Newtonian fluids, including Mohamadi et al [1]. In a study by Benos et al. [2], the flow of Casson fluid over a stretching sheet under the influence of a uniform magnetic field was explored. The study also considered the effects of thermal radiation and heat transfer rate on dual solutions for both time-dependent and independent two-dimensional magnetohydrodynamic flow of Casson fluid. Kataria and Harshad [3] studied the passage of time-dependent Casson fluid flow with natural convection in the presence of a transverse magnetic field on an oscillating vertical plate. Malathy et al. [4] conducted a study on the impact of an applied magnetic field, thermal conditions, and species concentration on the flow, heat, and mass transfer characteristics of a Casson fluid over a vertical permeable stretching sheetA study was conducted to analyze heat transfer and entropy generation in the presence of slip boundary conditions. The research focused on the flow of nano-refrigerant with a constant wall heat flux. In some real-life scenarios, certain issues need to be addressed, such as boundary layer control, cooling of metallic plates, and metallurgy. The impact of a uniform magnetic field is significant in determining the thermal radiation effects on dual solutions, as highlighted by Hamid et al [5]. Ghadikolaei et al. [6] conducted a study on the heat transfer properties of a thin Newtonian fluid film flowing over a continuously moving horizontal stretching sheet. They also considered the influence of Lorentz forces, radiation, heat sources, and slip boundary conditions. The purpose of the study was to showcase the impact of fluid flow on a stretching sheet which can be relevant to various technical fields such as polymer extrusion and hot rolling. . In a study conducted by Kavita et al. [7], they investigated how heat transfer affects the oscillatory flow of an electrically conducting Jeffrey fluid within a channel. The amount of heat emitted from the wall and the transport phenomenon are influenced by the increase in temperature, which leads to a reduction in the fluid's viscosity within the momentum boundary layer. Therefore, to accurately predict the flow characteristics and rates of heat transfer, the viscosity of the fluid must be a function of temperature. Ramesh and Devakar [8] conducted a study on the impact of non-uniform wall temperature and velocity slip effects on fluid under the influence of a traverse magnetic field on the lower plate. They configured a vertical channel with suction/injection effects for a time-dependent oscillatory flow and analyzed the primary fluid flow features for velocity and temperature profiles in detail. The study included the analysis of fundamental flow types, namely Couette, Poiseuille, and generalized Couette flow. Nadeem et al. [9] have examined the magnetohydrodynamic boundary layer flow of a Casson fluid over a shrinking sheet with exponential permeability. The slip and thermal radiation effects on Casson fluid over a stretching surface were thoroughly examined through the utilization of the homotropy analysis method. The research focused on the significance of studying heat and mass transfer with chemical reaction in various engineering and industrial processes. This study holds practical importance in industries such as electric power, chemical, and food processing. A group of researchers suggested a study to investigate the fluid flow behavior on a wavy surface with concurrent consideration of chemical reactions and heat source effects. Their study indicated that the oscillatory pressure gradient across the channel contributes to the unsteady flow of the fluid. The researchers also highlighted the importance of heat transport systems to handle varying oscillatory flow rates. Among these studies by Swati et al. [10] and Muthuraj and Srinivas [11].

The study of oscillatory Magnetohydrodynamic flow of a viscous fluid within a porous channel filled with porous media has significant importance in various physiological streams and engineering applications. These applications include blood flow in arteries, geothermal energy

extraction, petroleum engineering, nuclear reactors, and more. The transient or oscillatory flow of rheological fluids in channels is of great interest for natural and technological applications. For instance, the semi-intermittent bloodstream in the cardiovascular framework can be portrayed by the pressure and flow rate beats. Disturbances in the local stream of the blood vessels can cause various diseases associated with the vascular system. In specialized applications like inkjet printing, fast switching between the "no flow" and "flow" of a non-Newtonian fluid is required.

Peristaltic mechanism refers to the movement of fluid within a flexible tube through a progressive wave of either contraction or expansion along its length. The study of peristaltic flows is of great significance not only in biomedical and engineering sciences but also due to the intriguing mathematical aspects presented by the governing equations. These studies have practical implications in various biological processes such as urine transport, movement of chyme in the gastrointestinal tract, spermatozoa transport in the male reproductive tracts, ovum movement in the fallopian tube, lymph transport in lymphatic vessels, and vasomotion in small blood vessels. Additionally, the principle of peristalsis is utilized in devices like roller and finger pumps, as well as in the fabrication of biomechanical instruments like the heart-lung machine. The peristaltic movement is first examined by Latham [12]. Srivastava [13] investigated the transformation of a rigid frame into a curved shape due to the instability of liquid flow. They analyzed the Casson model about the peristaltic movement of blood and discovered that pressure variations are lower in cases of uneven geometry compared to uniform geometry. Kumar and Sivaraj [14] have provided a summary of their analysis on the result of the transfer of high temperature and slip in steady flows of viscous fluid. They focused on the magnetohydrodynamic flow over a vertical cone and flat plate with variable viscosity where there was a significant combination of heat and mass transfer. In their study, they emphasized the dependence of mass transfer of the species on the chemical reaction endpoint. Narla et al. [15] also discussed the modeling of transient hydrodynamic magneto-mediated peristaltic pumping of electroconductor viscoelastic fluids in a deformable curved channel. Several researchers continue to investigate and explore this field Chemical reactions between foreign masses and fluids are common in many chemical engineering processes, including polymer production ceramics and glassware manufacturing, and food processing [16]. Ajithkumar et al. [17] investigated the MHD peristaltic transport of a radiative Casson fluid with both homogeneous and heterogeneous chemical processes via a porous medium in an inclined flexible channel. Also, they took into account the Hall currents and the consequences of heat generation.

The current project aims to determine the effects of an asymmetric channel on the MHD oscillatory flow of a Non-Newtonian Casson fluid in the presence of the heat source or sink, thermal radiation, suction or injection, chemical reaction, and porous media. Exact solutions to the dimensionless governing equations are found through solving them. Analysis has been done on how various physical parameters affect the momentum, thermal, and solutal profiles of the Casson fluid. Many use thick monolayers of surfaces covered with the hydrophobic substance octadecyltrichlorosilane, and thin oil films adhered to moving plates.

2. Mathematical formulation

Let's consider the flow of an electrically conducting viscous fluid (Casson model) that is incompressible and time-dependent. The flow occurs in an asymmetric wavy channel, where the x-direction runs through the center of the channel and the y-direction is perpendicular to the x-direction, see Fig. 1. The induced magnetic field is thought to be insignificant in comparison to the applied magnetic field because of the extremely low magnetic Reynolds number. Additionally, The low velocities usually found in free convection flows and oscillatory flows allow us to ignore the effects of viscous dissipation, Joule heating, and porous medium-resistant heating.

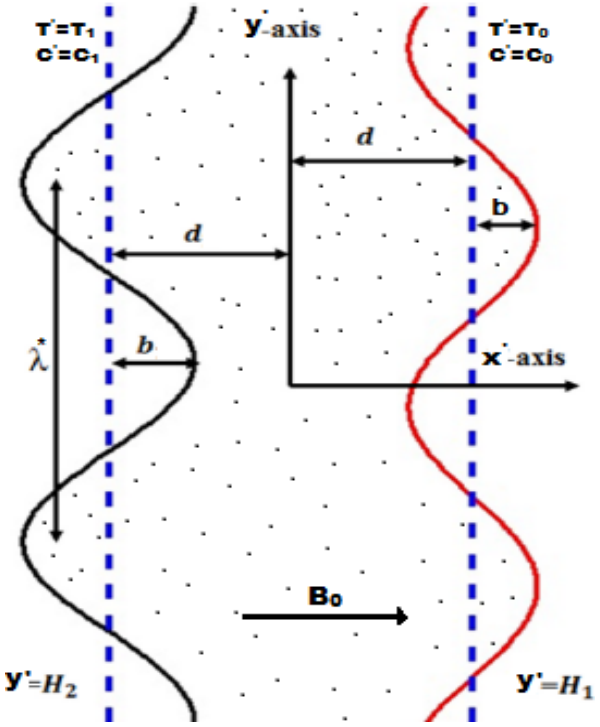

Fig. 1. Model schematic diagram.

By employing the Boussinesq approximation, the governing equations of the flow are given as:

$$\rho\left(u'\frac{\partial u'}{\partial x'}+v'\frac{\partial u'}{\partial y'}+\frac{\partial u'}{\partial t'}\right) = \frac{-\partial p'}{\partial x'}+\mu\left(1+\frac{1}{\beta}\right)\left(\frac{\partial^2 u'}{\partial x'^2}+\frac{\partial^2 u'}{\partial y'^2}\right)-\frac{\mu}{k^*}\left(1+\frac{1}{\beta}\right)u'-\sigma B_0^2 u' + \rho\beta_T g(T'-T_0)+\rho\beta_C g(C'-C_0), \tag{1}$$

$$\rho\left(u'\frac{\partial V'}{\partial x'}+v'\frac{\partial V'}{\partial y'}+\frac{\partial V'}{\partial t'}\right)=\frac{-\partial p'}{\partial y'}+\mu\left(1+\frac{1}{\beta}\right)\left(\frac{\partial^2 V'}{\partial x'^2}+\frac{\partial^2 V'}{\partial y'^2}\right), \tag{2}$$

$$\rho C_p\left(u'\frac{\partial T'}{\partial x'}+v'\frac{\partial T'}{\partial y'}+\frac{\partial T'}{\partial t'}\right)=K\left(\frac{\partial^2 T'}{\partial x'^2}+\frac{\partial^2 T'}{\partial y'^2}\right)-\frac{\partial q_r}{\partial y'}+Q_0(T'-T_0), \tag{3}$$

$$u'\frac{\partial C'}{\partial x'}+v'\frac{\partial C'}{\partial y'}+\frac{\partial C'}{\partial t'}=D\left(\frac{\partial^2 C'}{\partial x'^2}+\frac{\partial^2 C'}{\partial y'^2}\right)-K_1(C'-C_0). \tag{4}$$

The boundary conditions for the present analysis are

$$\mathrm{u}'=0\,,\mathrm{T}'=\mathrm{T}_0\,,C'=C_0 \quad at\ y'=H_1\,,$$
$$\mathrm{u}'=0,\mathrm{T}'=\mathrm{T}_1\,,C'=C_1 \quad at\ y'=H_2\,. \tag{5}$$

Here $\mathrm{T}_1>\mathrm{T}_0\ and\ \mathrm{C}_1>\mathrm{C}_0$.

According to the assumption that fluid is optically thin, the radiative heat flow is given by

$$\frac{\partial q_r}{\partial y'}=4\alpha^2(\,\mathrm{T}'-\mathrm{T}_0\,). \tag{6}$$

The velocity, the temperature and the concentration fields of the present problem are

$$v=(u'(y',t'),-\mathrm{v}_0,0),\mathrm{T}'=\mathrm{T}'(\mathrm{y}',\mathrm{t}'),\mathrm{C}'=\mathrm{C}'(\mathrm{y}',\mathrm{t}'). \tag{7}$$

Under the above assumptions and with the help of Eqs. (6) and (7), the equation for momentum, energy and concertation can be written as:

$$\rho\left(\frac{\partial u'}{\partial t'}-v_0\frac{\partial u'}{\partial y'}\right)=\frac{-\partial p'}{\partial x'}+\mu\left(1+\frac{1}{\beta}\right)\frac{\partial^2 u'}{\partial y'^2}-\frac{\mu}{k^*}\left(1+\frac{1}{\beta}\right)u'-\sigma B_0^2u'+\rho\beta_T g(T'-T_0)+\rho\beta_C g(C'-C_0), \tag{8}$$

$$0=-\frac{\partial p'}{\partial y'}, \tag{9}$$

$$\rho\left(\frac{\partial T'}{\partial t'}-v_0\frac{\partial T'}{\partial y'}\right)=K\left(\frac{\partial^2 T'}{\partial y'^2}\right)+4\alpha^2(T'-T_0)+Q_0(T'-T_0), \tag{10}$$

$$\left(\frac{\partial C'}{\partial t'}-v_0\frac{\partial C'}{\partial y'}\right)=D\left(\frac{\partial^2 C'}{\partial y'^2}\right)-K_1(C'-C_0). \tag{11}$$

With the following boundary conditions:

$$\mathrm{u}'=0,\mathrm{T}'=\mathrm{T}_0\,,C'=C_0 \quad at\ y'=H_1,$$
$$\mathrm{u}'=0,\mathrm{T}'=\mathrm{T}_1,C'=C_1 \quad at\ y'=H_2\,. \tag{12}$$

Dimensionless variables are given by

$$x = \frac{x'}{d}\ , y = \frac{y'}{d}\ , u = \frac{u'\,d}{\mu}, h_1 = \frac{H_1}{d}, h_2 = \frac{H_2}{d}, t = \frac{t'\mu}{d^2}, a = \frac{b}{d}, p = \frac{p'd^2}{\rho\mu^2}$$

$$Da = \frac{k^*}{d^2}\ , G_t = \frac{\beta_T g d^3 (T_1 - T_0)}{\mu^2}\ , G_c = \frac{\beta_c g d^3 (C_1 - C_0)}{\mu^2}\ , Pr = \frac{\rho\mu C_p}{k}$$

$$\theta = \frac{T'-T_0}{T_1{}'-T_0}, \phi = \frac{C'-C_0}{C_1{}'-C_0}, S = \frac{v_0 d}{\mu}, kr = \frac{K_1 d^2}{\mu}, Nr = \frac{4\alpha^2 d^2}{\rho\mu C_p}, Ha^2 = \frac{\sigma B_0^2 d^2}{\rho\mu},$$

$$Sc = \frac{D}{\mu}, Q = \frac{Q_0 d^2}{\rho\mu C_p}, \alpha_1 = \frac{2\pi d}{\lambda}, \alpha_2 = \frac{2\pi c d^2}{\mu}. \tag{13}$$

Therefore, the non-dimensional equations are formatted as follows:

$$\frac{\partial u}{\partial t} - S\frac{\partial u}{\partial y} = \frac{-\partial p}{\partial x} + \left(1 + \frac{1}{\beta}\right)\frac{\partial^2 u}{\partial y^2} - u\left(\frac{1}{Da}\left(1 + \frac{1}{\beta}\right) + Ha^2\right) + G_t\theta + G_c\phi, \tag{14}$$

$$\frac{\partial \theta}{\partial t} - S\frac{\partial \theta}{\partial y} = \frac{1}{Pr}\frac{\partial^2 \theta}{\partial y^2} + (Nr + Q)\theta, \tag{15}$$

$$\frac{\partial \phi}{\partial t} - S\frac{\partial \phi}{\partial y} = Sc\left(\frac{\partial^2 \phi}{\partial y^2}\right) - kr\phi. \tag{16}$$

The boundary conditions are in dimensionless:

$$u = 0, \theta = 0, \phi = 0 \quad \text{at} \quad y = h_1,$$

$$u = 0, \theta = 1, \phi = 1 \quad \text{at} \quad y = h_2. \tag{17}$$

The walls of the peristaltic channel are given by

$$H_1 = d + b\cos\frac{2\pi}{\lambda^*}(x' - ct')\ ,$$

$$H_2 = -d - b\cos\left(\frac{2\pi}{\lambda^*}(x' - ct') + \varphi\right), \tag{18}$$

where $\varphi \in [0, \pi]$, in which $\varphi = 0$ indicates a symmetric channel with out-of-phase waves and $\varphi = \pi$ refers to that with in-phase waves. Furthermore, b, d and φ achieve the following relation $b^2 + b\,cos\varphi \leq 2d^2$.

In dimensionless:

$$h_1 = 1 + a\cos(\alpha_1 x - \alpha_2 t),$$

$$h_2 = -1 - a\cos((\alpha_1 x - \alpha_2 t) + \varphi). \tag{19}$$

3. Method of solution

Solving Eqs. (14) -(16) by the method of separation of variables. It is assumed that the oscillatory pressure gradient, velocity, temperature and concentration take the following form:

$$\begin{aligned} &\frac{-dP}{dx} = \lambda e^{i\omega t}, u(y,t) = u_0(y)e^{i\omega t}, \\ &\theta(y,t) = \theta_0(y)e^{i\omega t}, \phi(y,t) = \phi_0(y)e^{i\omega t}, \end{aligned} \tag{20}$$

Applying (20) in Eqs. (14)-(17), we get the following set of ordinary differential equations:

$$\left(1+\frac{1}{\beta}\right)u_0'' - u_0\left(\frac{1}{Da}\left(1+\frac{1}{\beta}\right) + Ha^2 + iw\right) + Su_0' = -\lambda - G_t\theta_0 - G_c\phi_0, \tag{21}$$

$$\frac{1}{Pr}\theta_0'' + (Nr + Q - iw)\theta_0 + S\theta_0' = 0, \tag{22}$$

$$Sc\phi_0'' + S\phi_0' - (Kr + iw)\phi_0 = 0. \tag{23}$$

The corresponding boundary conditions are

$$\begin{aligned} &u_0 = 0, \theta_0 = 0, \phi_0 = 0 at\ y = h_1, \\ &u_0 = 0, \theta_0 = 1, \phi_0 = 1 at\ y = h_2. \end{aligned} \tag{24}$$

Eqs. (21)-(23) concerning the boundary conditions (24) are solved by using the command DSolve[eqn, y, x]. The axial velocity, temperature, and concentration are obtained as:

$$\begin{aligned} &\text{solVel} = \text{DSolve}[\{\text{a1u0"}[y] + S\text{u0}'[y] - \text{a2u0}[y] = \\ &\qquad = -\lambda - \text{Gt}\theta 0[y] - \text{Gc}\phi 0[y], \text{u0}[\text{h1}] == 0, \text{u0}[\text{h2}] == 0\}, \text{u0}[y], y]; \end{aligned} \tag{25}$$

$$\begin{aligned} &\{\{(512\ \text{a1}^5\ (-2\ \text{A0 a1 a2}^4\ e^{\frac{\cdots 1 \cdots}{2\ \text{a1}} + \frac{1}{2}(\cdots 1 \cdots)y}\ \text{Gt m1} + \cdots 1090 \cdots + 2\ \text{m1 m2 m3 m4 S}^4 \\ &\sqrt{4\ \text{a1 a2} + \text{S}^2}\ \lambda))/(\sqrt{4\ \text{a1 a2} + \text{S}^2}\ (-\text{S} + \sqrt{4\ \text{a1 a2} + \text{S}^2})\ (-2\ \text{a1 m1-S} + \sqrt{4\ \text{a1 a2} + \text{S}^2})\ \cdots 6 \cdots \\ &(2\ \text{a1 m3+S} + \sqrt{4\ \text{a1 a2} + \text{S}^2})\ (2\ \text{a1 m4+S} + \sqrt{4\ \text{a1 a2} + \text{S}^2}))) + \cdots 1 \cdots / \cdots 1 \cdots + (e^{\cdots 1 \cdots}\ (\\ &\cdots 1 \cdots))/(2\ \cdots 6 \cdots\ \sqrt{\cdots 1 \cdots + \cdots 1 \cdots})\}, \\ &\{\{\{\text{large output}\ ,\ \text{show less}\ ,\ \text{show more}\ ,\ \text{show all}\ ,\ \text{set size limit...}\ \}\}\}\} \end{aligned} \tag{26}$$

For the sake of brevity, the mathematical expression for velocity is too long to be written down.

$$\begin{aligned} &\text{solTemp} = \text{DSolve}[\{\theta 0"[y] + S\text{Pr}\theta 0'[y] + \text{a3}\theta 0[y] == 0, \theta 0[\text{h1}] == 0, \theta 0[\text{h2}] = \\ &\qquad = 1\}, \theta 0[y], y]; \end{aligned} \tag{27}$$

$$\begin{aligned} &\theta = (e\text{^}(1/2\ \text{h1}(-\text{Pr}S + \sqrt{}(-4\text{a3} + \text{Pr\^{}2}\ S\text{\^{}2}\ ))) + 1/2(-\text{Pr}S - \sqrt{}(-4\text{a3} + \\ &\text{Pr\^{}2}\ S\text{\^{}2}\ ))y) - e\text{^}(1/2\ \text{h1}(-\text{Pr}S - \sqrt{}(-4\text{a3} + \text{Pr\^{}2}\ S\text{\^{}2}\ )) + 1/2(-\text{Pr}S + \\ &\sqrt{}(-4\text{a3} + \text{Pr\^{}2}\ S\text{\^{}2}\ ))y))/(e\text{^}(1/2\ \text{h2}(-\text{Pr}S - \sqrt{}(-4\text{a3} + \text{Pr\^{}2}\ S\text{\^{}2}\ )) + 1/ \\ &2\ \text{h1}(-\text{Pr}S + \sqrt{}(-4\text{a3} + \text{Pr\^{}2}\ S\text{\^{}2}\ ))) - e\text{^}(1/2\ \text{h1}(-\text{Pr}S - \sqrt{}(-4\text{a3} + \\ &\text{Pr\^{}2}\ S\text{\^{}2}\ )) + 1/2\ \text{h2}(-\text{Pr}S + \sqrt{}(-4\text{a3} + \text{Pr\^{}2}\ S\text{\^{}2}\ ))), \end{aligned} \tag{28}$$

$$\text{solConc} = \text{ExpandAll}[\text{DSolve}[\{\text{Sc}\phi 0''''[y] + S\phi 0'[y] - \text{a4}\phi 0[y] == 0, \phi 0[\text{h1}] == 0, \phi 0[\text{h2}] == 1\}, \phi 0[y], y]]; \tag{29}$$

$$\begin{aligned}\phi = {} & e\text{^}(-\text{h1}S/2\text{Sc} + (\text{h1}\sqrt{(S\text{^}2 + 4\text{a4Sc})})/2\text{Sc} - Sy/2\text{Sc} - (\sqrt{(S\text{^}2 + 4\text{a4Sc})}\, y)/2\text{Sc})/(e\text{^}(-\text{h1}S/2\text{Sc} - \text{h2}S/2\text{Sc} + (\text{h1}\sqrt{(S\text{^}2 + 4\text{a4Sc})})/2\text{Sc} - (\text{h2}\sqrt{(S\text{^}2 + 4\text{a4Sc})})/2\text{Sc}) - e\text{^}(-\text{h1}S/2\text{Sc} - \text{h2}S/2\text{Sc} - (\text{h1}\sqrt{(S\text{^}2 + 4\text{a4Sc})})/2\text{Sc} + (\text{h2}\sqrt{(S\text{^}2 + 4\text{a4Sc})})/2\text{Sc})) - e\text{^}(-\text{h1}S/2\text{Sc} - (\text{h1}\sqrt{(S\text{^}2 + 4\text{a4Sc})})/2\text{Sc} - Sy/2\text{Sc} + (\sqrt{(S\text{^}2 + 4\text{a4Sc})}\, y)/2\text{Sc})/(e\text{^}(-\text{h1}S/2\text{Sc} - \text{h2}S/2\text{Sc} + (\text{h1}\sqrt{(S\text{^}2 + 4\text{a4Sc})})/2\text{Sc} - (\text{h2}\sqrt{(S\text{^}2 + 4\text{a4Sc})})/2\text{Sc}) - e\text{^}(-\text{h1}S/2\text{Sc} - \text{h2}S/2\text{Sc} - (\text{h1}\sqrt{(S\text{^}2 + 4\text{a4Sc})})/2\text{Sc} + (\text{h2}\sqrt{(S\text{^}2 + 4\text{a4Sc})})/2\text{Sc})),\end{aligned} \tag{30}$$

where

$a1 = 1 + 1/\beta,$
$a2 = 1/Da\ (1 + 1/\beta) + Ha2 + i\omega,$
$a3 = Nr + Q - i\omega,$
$a4 = kr + i\omega,$ and $i = \sqrt{-1}.$

4. Results and discussion

An investigation has been conducted on the flow of a highly viscous fluid (Casson fluid) inside an asymmetric wavy channel embedded in a porous media in the presence of heat source/sink, suction /injection, thermal radiation, and chemical reaction. The flow, caused by free convection and increasing pressure gradients, occurs through a vertical channel. The study analyzes the influence of physical parameters such as β, ω, S, Ha, Da, λ, G_t, G_c, Pr, Q, Nr, Sc, and kr on the momentum, energy and solutal profiles of the Casson fluid. In all the graph calculations, $a = 0.4, b = 0.3, d = 1.1, x = 0.1$.

(a)

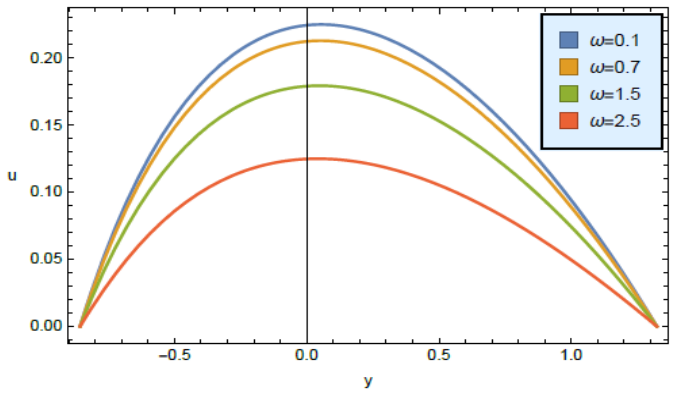

(b)

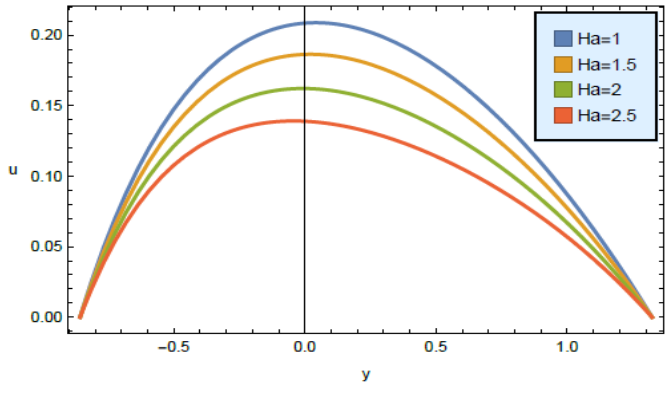

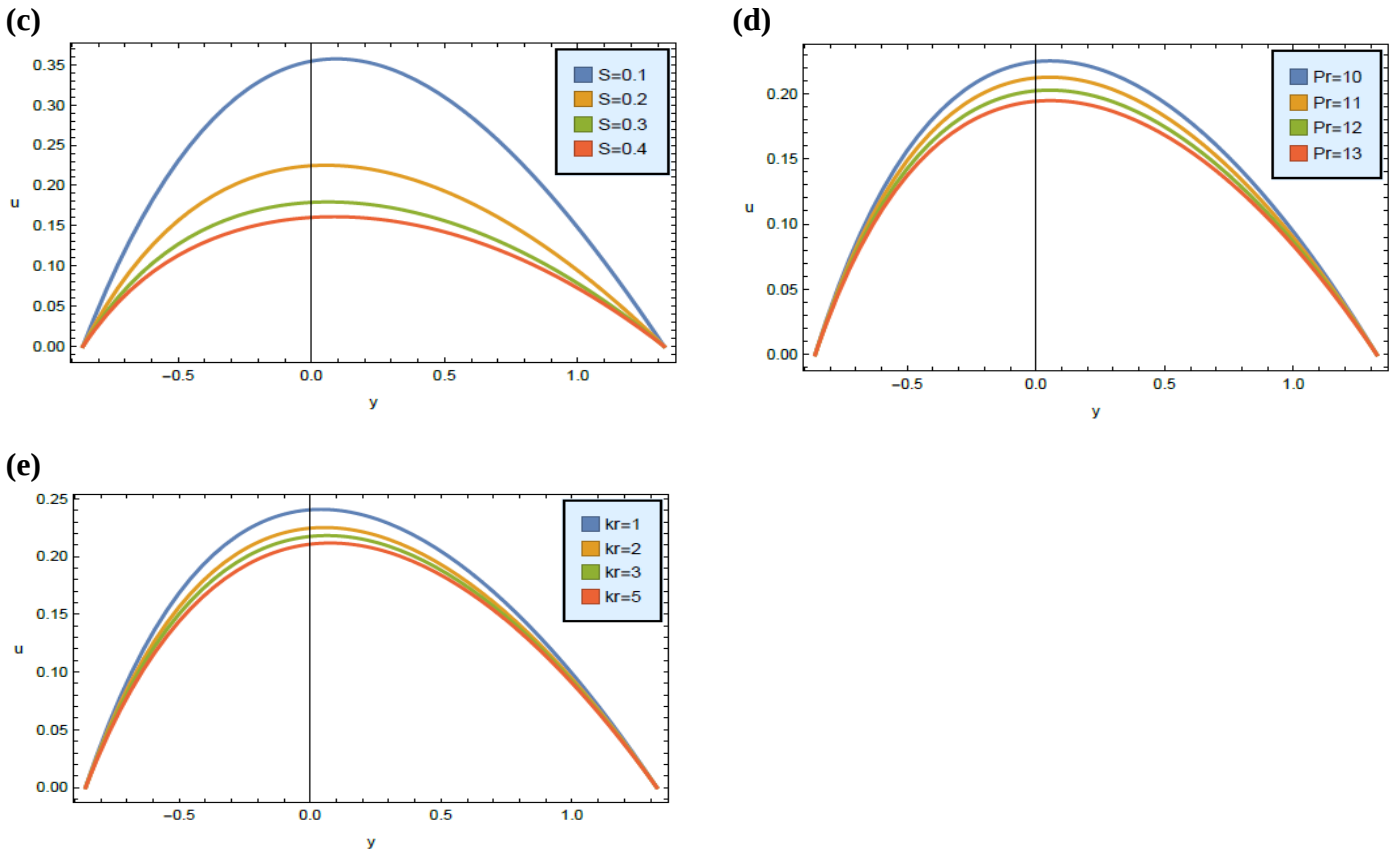

Fig. 2. Variation of velocity profile u with y for different values of (a) ω, (b) Ha, (c) S, (d) Pr, and (e) kr.

Effects of various physical parameters on velocity profiles:

The effect of the parameters on ω, Ha, S, Pr, and kr the velocity profile is shown in Figs. 2(a)-(e). In Fig. 2(a) The velocity tend to vary based on the frequency of oscillations. If the parameter mentioned here is increased, it results in a corresponding decrease in the velocity profile. In Fig. 2(b) The flow is highest when there is no magnetic field present, but as the Hartmann number increases, the velocity decreases. In Fig. 2(c) the velocity of fluid changes with increasing values of the parameter S. As the suction/injection parameter increases, the velocity of fluid at the surface of the cold medium decreases. This happens because of the injection of cold liquid particles and the hot liquid particles are simultaneously suctioned out of the channel. In Fig. 2(d) velocity decreases with the increase in Prandtl number Pr. In Fig. 2(e) the increase in chemical reaction parameter suppresses velocity distribution.

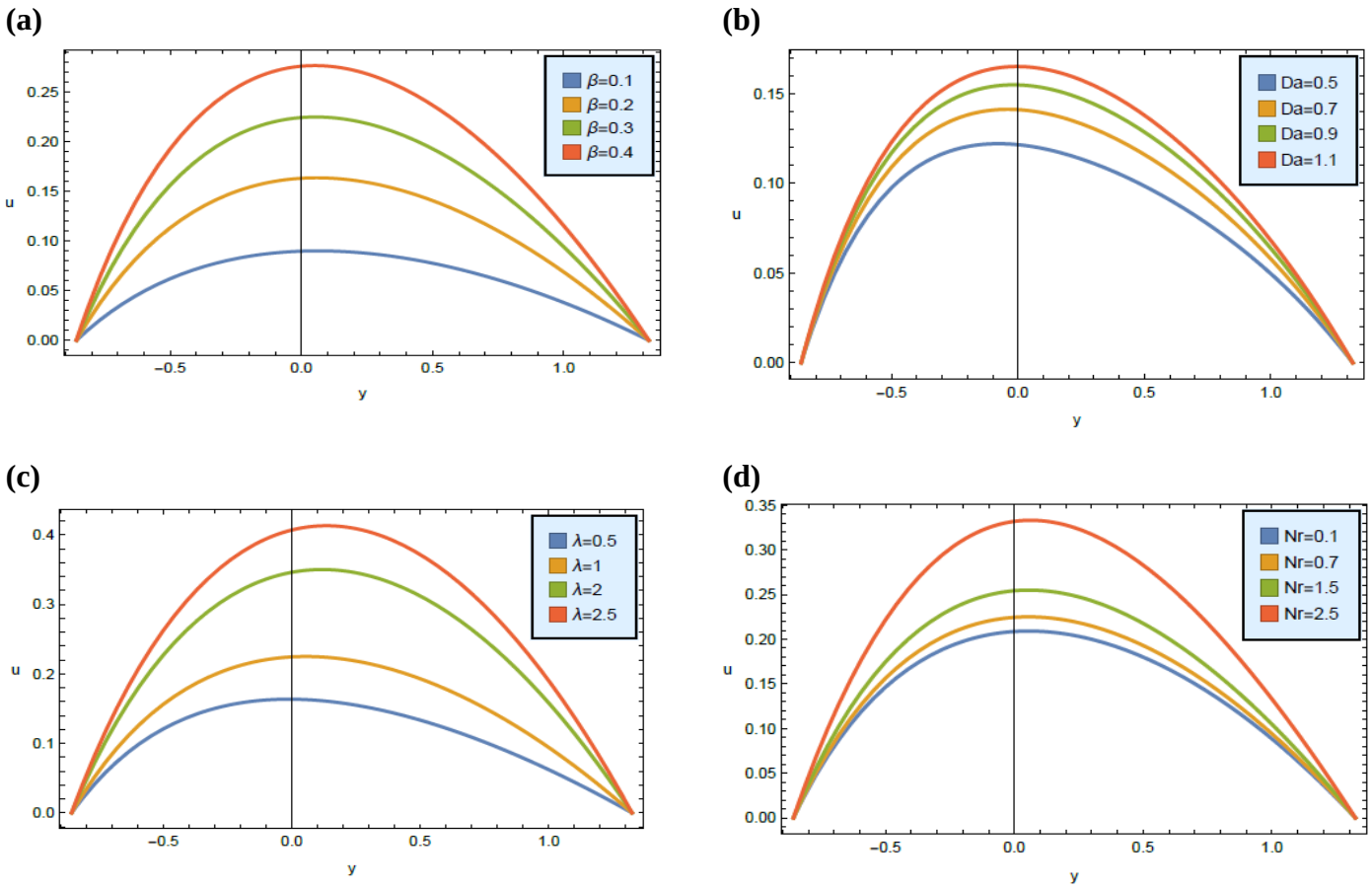

Fig. 3. Variation of velocity profile u with y for different values of (a) β, (b) Da, (c) λ, and (d) Nr.

Figs. 3(a)-(d) indicate the effect of various values of β, Da, λ, and Nr on the velocity distributions. In Fig. 3(a) the velocity of the fluid is increased by the presence of β. In Fig. 3(b), as Da increases the velocity becomes more pronounced. The reduction of physical barriers along the flow channel enables the fluid to move more freely, leading to an increase in fluid velocity. In Fig. 3 (c) the fluid flow is affected by the pressure gradient when fluid is pumped, the flow increases in the opposite direction of the gravitational force. In Fig. 3(d), when Nr is increased, it leads to a notable improvement in the thermal conditions of the fluid temperature. This results in an increase in the amount of fluid in the boundary layer due to the buoyancy effect, which in turn causes an acceleration in the velocity of the fluid.

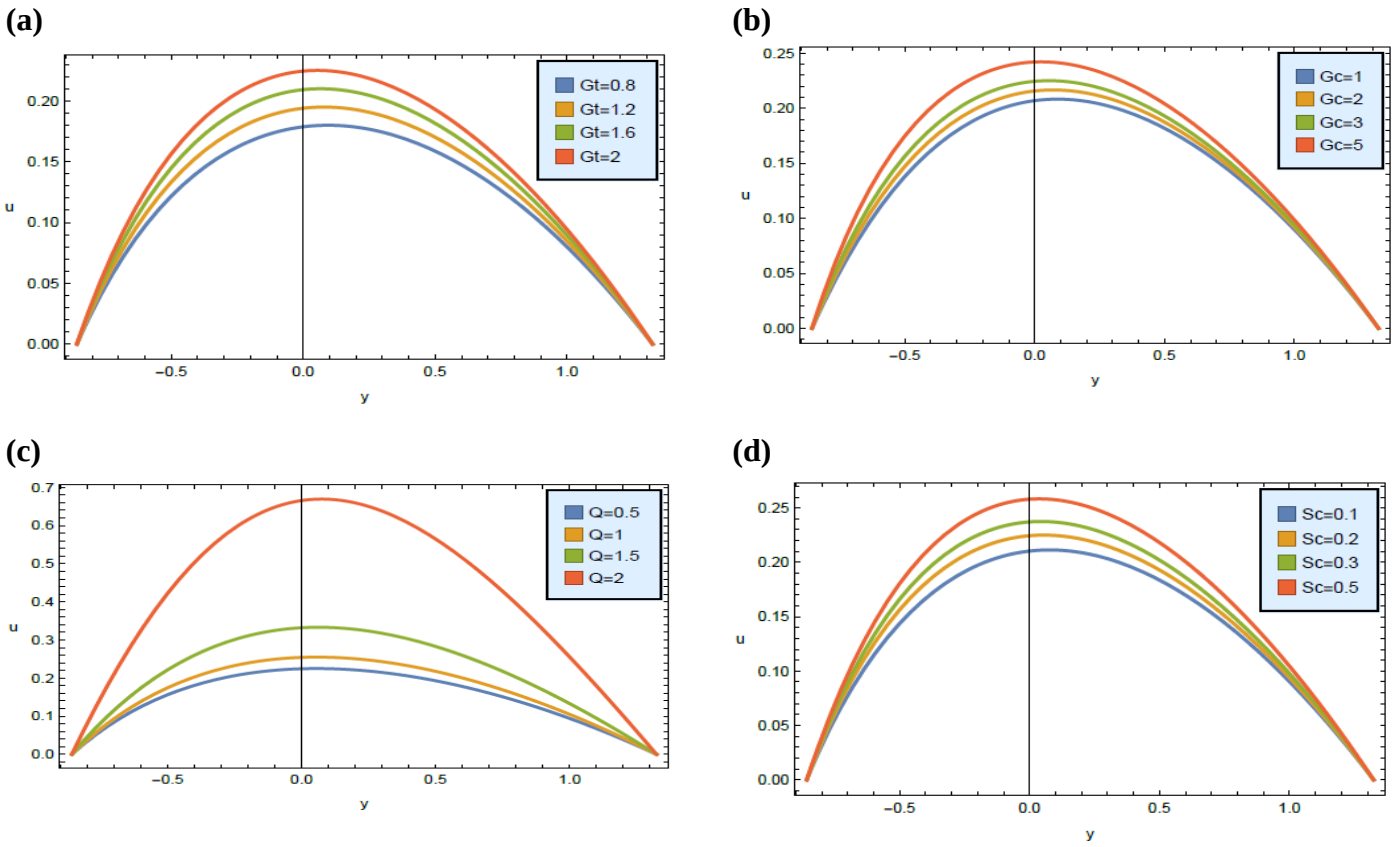

Fig. 4. Variation of velocity profile u with y for different values of (a) G_t, (b) G_c, (c) Q, and (d) Sc.

Figs. 4(a)-(d) exhibit the effect of altering values of G_t, G_c, Q, and Sc on velocity profile. In Fig. 4(a) the changes in fluid flow caused by heating ($G_t > 0$) can be explained by the buoyancy effect. As the Thermal Grashof number increases, the velocity profile increases as well. Conversely, when the parameter decreases due to cooling, the opposite effect occurs. In Fig. 4(b) the solutal Grashof number (Gc) is used to describe the relationship between the buoyancy force of a species and the hydrodynamic force caused by viscosity. It has been observed that an increase in the species buoyancy force results in a noticeable increase in fluid velocity, making the peak value more prominent. In Fig. 4(c) velocity increases when Q increases. In Fig. 4(d), as the Schmidt number Sc increases, the velocity is affected, resulting in a decrease in concentration. This decrease in concentration leads to a reduction in fluid velocity as the concentration buoyancy effects decrease.

Effects of various physical parameters on temperature profiles:

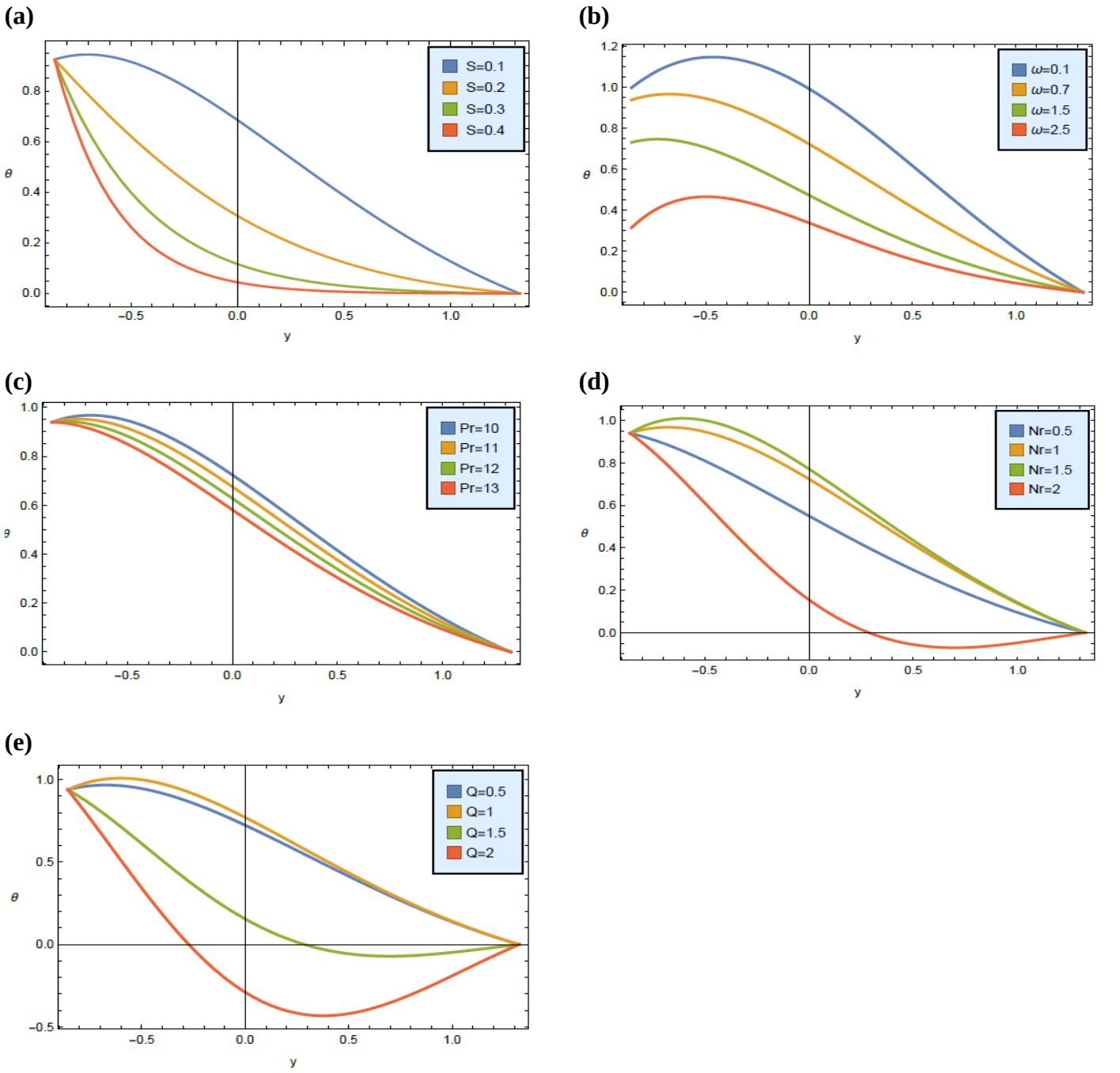

Fig. 5. Variation of temperature profile θ with y for different values of (a) S, (b) ω, (c) Pr, (d) Nr, and (e) Q.

Figs. 5(a)-(d) indicate the influence of parameters on the temperature distributions for varying values of S, ω, Pr, Nr, and Q. In Fig. 5(a) the temperature of the fluid does not evenly disperse across the channel. Increasing S on the heated surface causes a decrease in fluid temperature within the channel. As S increases, the flow of heat from the hot surface to the cold one causes a convex

pattern to emerge based on the rate of heat transfer. In Fig. 5(b), by increasing ω , θ through the channel decreases. In Fig. 5(c) the temperature is influenced by different values of Pr, which has the ability to restrict the temperature distribution. Pr measures the ratio of viscous force to thermal force and determines the relative importance of viscous dissipation compared to thermal dissipation. Moreover, a fluid with a low Pr tends to increase the rate of heat transfer. In Fig. 5(d), when the Nr is increased, it leads to a notable rise in the fluid temperature, resulting in increased fluid in the boundary layer due to buoyancy effect. This, in turn, causes an increase in fluid velocity. In Fig. 5(e) depicts the variation of temperature concerning Q. It is observed that the increase in Q parameter decreases the temperature profile.

Effects of various physical parameters on concentration profiles:

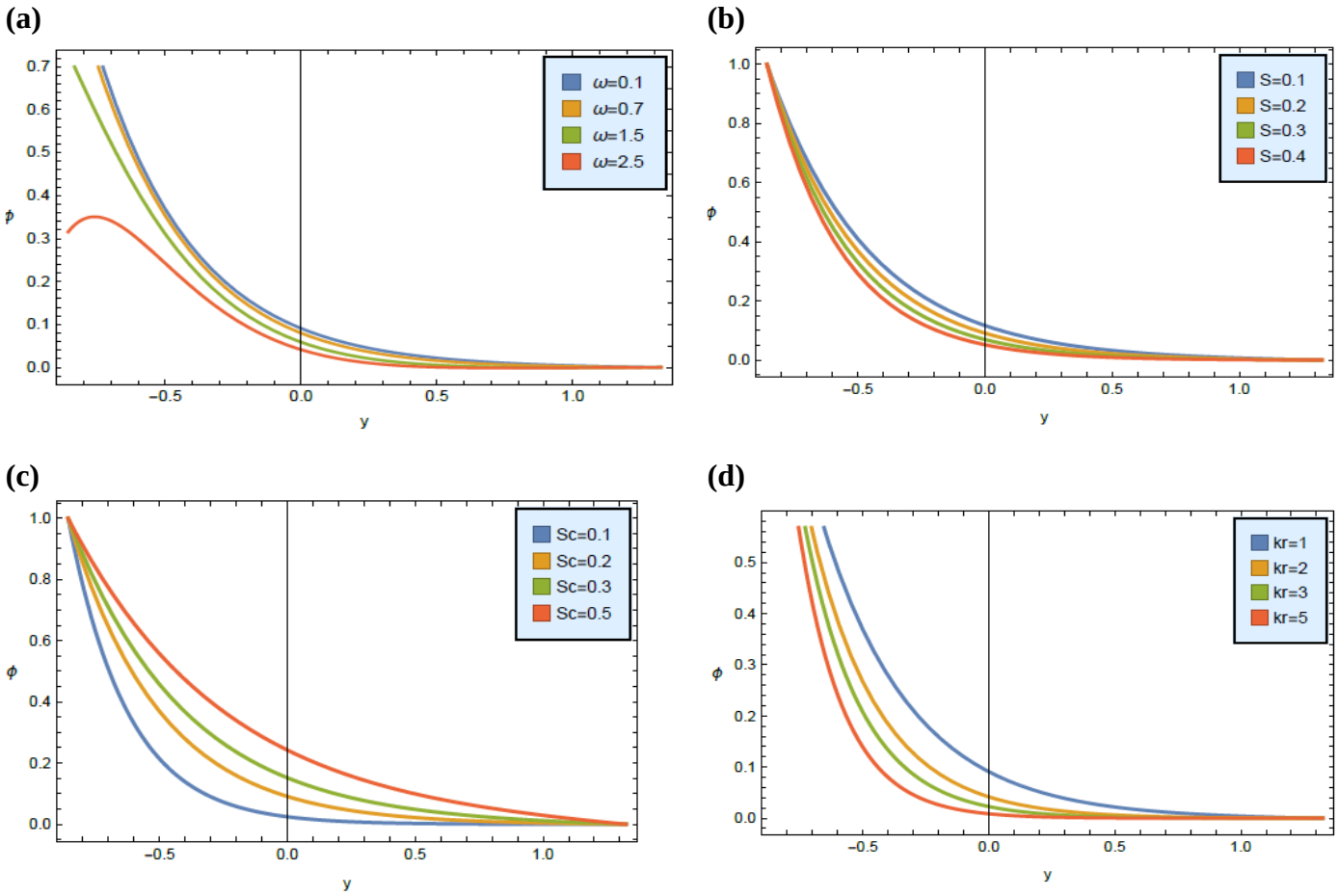

Fig. 6. Variation of concentration profile ϕ with y for different values of (a) ω, (b) S, (c) Sc, and (d) kr.

The concentration ϕ graphs are outlined for ω, S, Sc, and kr in Figs. 6(a)-(d). In Fig. 6(a), ω increasing lead to concentration profile decreasing. In Fig. 6(b) when S increases, concentration profile decreases. In Fig. 6(c) as Sc increases, the rate of mass transfer increases, resulting in a inecrease in concentration profiles. In Fig. 6(d) increasing kr, suppresses the concentration.

5. Conclusions

A theoretical analysis has been conducted on the Casson fluid flow in a wavy channel with heat and mass transfers. Prominent parameters for the velocity, temperature, and concentration profiles, which are evaluated by the graph have been provided. with the help of the MATHEMATICA 14 software. The results were developed graphically. Our findings are as follows:

- When the Hartmann number is increased, velocity is reduced.
- As thermal radiation parameter is increased, it leads to an acceleration in the velocity of the fluid.
- The increase in heat source/sink parameter and Prandtl number decrease the temperature profile.
- The frequency of oscillation, chemical reaction, and suction/injection parameter reduce the concentration profile of the Casson fluid.
- The Schmidt number boost the fluid concentration.

References

1. S. Mohamadi, M.H. Yazdi, E. Solomin, A. Fudholi, K. Sopian, P.L. Chong (2021). Heat transfer and entropy generation analysis of internal flow of nanorefrigerant with slip condition at wall. Therm. Sci. Eng. Prog. 22 100829.
2. L.T. Benos, U.S. Mahabaleshwar, P.H. Sakanaka, I.E. Sarris (2019). Thermal analysis of the unsteady sheet stretching subject to slip and magnetohydrodynamic effects, Therm. Sci. Eng. Prog. 13 100367.
3. H. Kataria, H. Patel (2018). Heat and mass transfer in magnetohydrodynamic (MHD) Casson fluid flow past over an oscillating vertical plate embedded in porous medium with ramped wall temperature. Propul. Power Res. 7 (3) 257-267.
4. T. Malathy, S. Srinivas, A.S. Reddy (2017). Chemical reaction and thermal radiation effects on MHD pulsatile flow of an Oldroyd-B fluid in a porous medium with slip and convective boundary conditions. J. Porous Media 20 (4) 287–301.
5. M. Hamid, M. Usman, Z.H. Khan, R. Ahmad, W. Wang (2019) . Dual solutions and stability analysis of flow and heat transfer of Casson fluid over a stretching sheet, Phys. Lett. A 383 (20) 2400–2408.
6. S.S. Ghadikolaei, K. Hosseinzadeh, M. Yassari, H. Sadeghi, D.D. Ganji (2018). Analytical and numerical solution of non-Newtonian second-grade fluid flow on a stretching sheet, Therm. Sci. Eng. Prog. 5 309–316.
7. K. Kavita, K.R. Prasad, B.A. Kumari (2012). Influence of heat transfer on MHD oscillatory flow of Jeffrey fluid in a channel. Adv. Appl. Sci. Res. 3 2232–2312.

8. K. Ramesh, M. Devakar (2015). Some analytical solutions for flows of Casson fluid with slip boundary conditions, Ain Shams Eng. J. 6 (3) 967–975.
9. S. Nadeem, R. Ul Haq, C. Lee (2012). MHD flow of a Casson fluid over an exponentially shrinking sheet. Sci. Iran. 19(6) 1550–1553.
10. S. Mukhopadhyay, P.R. De, K. Bhattacharyya, G.C. Layek(2013) . Casson fluid flow over an unsteady stretching surface, Ain Shams Eng. J. 4 (4) 933–938.
11. R. Muthuraj, S. Srinivas (2010). A note on heat transfer to MHD oscillatory flow in an asymmetric wavy channel, Int. Commun. Heat Mass Transfer 37 (9) 1255–1260
12. Latham TW. Fluid Motion in a Peristaltic Pump Master's Thesis. Cambridge, MA, USA: MIT; 1966.
13. L.M. Srivastava, V.P. Srivastava (1984). Peristaltic transport of blood: Casson model-II. J. Biomech. 17 821–830.
14. Kumar B Rushi, R. Sivaraj (2013). Heat and mass transfer in MHD viscoelastic fluid flow over a vertical cone and flat plate with variable viscosity. Int J Heat Mass Transfer. 56 370–379.
15. V.K. Narla, D. Tripathi, O.A. Bég (2018). Modeling transient magneto hydrodynamic peristaltic pumping of electroconductive viscoelastic fluids through a deformable curved channel. J. Eng. Math. 111 127–143.
16. C. Bridges, K.R. Rajagopa (2006). Pulsatile flow of a chemically-reacting nonlinear fluid. Comput. Math. Appl. 52 (6–7) 1131–1144.
17. M. Ajithkumar, K. Vajravelu, G. Sucharitha, P. Lakshminarayana (2024). Investigation of a conducting Casson fluid flow through a porous flexible microfluidic channel with catalytic effects: application in pharmaceutical fluid processing. Eur. Phys. J Plus 139 265.